
Vision Language Models Cannot Reason About Physical Transformation

Dezhi Luo^{*1} Yijiang Li^{*2} Maijunxian Wang³ Tianwei Zhao⁴ Bingyang Wang⁵ Siheng Wang⁶
 Pinyuan Feng⁷ Pooyan Rahmazadehgervi⁸ Ziqiao Ma¹ Hokin Deng⁹

Abstract

Understanding physical transformations is fundamental for reasoning in dynamic environments. While Vision Language Models (VLMs) show promise in embodied applications, whether they genuinely understand physical transformations remains unclear. We introduce *Conservation-Bench* evaluating *conservation*—whether physical quantities remain invariant under transformations. Spanning four properties with paired conserving/non-conserving scenarios, we generate 23,040 questions across 112 VLMs. Results reveal systematic failure: performance remains near chance with improvements on conservation tasks accompanied by drops on controls. Control experiments show strong textual priors favoring invariance, yet models perform worse with visual content. Neither temporal resolution, prompting, nor curated sampling helps. These findings show that current VLMs fail to maintain transformation-invariant representations of physical properties across dynamic scenes.

1. Introduction

Recent advances in Vision Language Models (VLMs) (Zhang et al., 2024c; Radford et al., 2021; Alayrac et al., 2022; Li et al., 2023) have demonstrated remarkable capabilities of perception (Wang et al., 2024; Chen et al., 2025; Jiang et al., 2025; Team et al., 2025; Cheng et al., 2024b), reasoning (Zhang et al., 2024b; Xu et al., 2024; Cheng et al., 2024a), and visual commonsense understanding (Zellers et al., 2019; Park et al., 2020). These capabilities hold promise for real-world applications (Brohan et al., 2023), particularly in embodied tasks (Driess et al., 2023; Nasiriany et al., 2024) that demand

a genuine understanding of the physical world and its underlying properties (Chow et al., 2025b; Gao et al., 2024a). Yet it remains unclear whether VLMs possess a true understanding of physical principles or the capacity to operate reliably in embodied physical environments.

A key factor in human intelligence that enables successful navigation in an embodied, physically grounded world is the ability to understand and reason about physical transformations (Piaget, 1950; 1952; 1965; Baillargeon et al., 1985; 1990; Baillargeon, 1987; 1986; Spelke et al., 1992; Baillargeon & Carey, 2012; Bear et al., 2021; Piloto et al., 2022). This capacity includes tracking objects over time (Spelke et al., 1994; 1995), managing occlusions (Gredebäck & von Hofsten, 2004), and adapting to dynamic environments (Allen et al., 2020). While there are benchmarks evaluating physically plausible video generation (Motamed et al., 2025; Meng et al., 2024; Yang et al., 2025; Liu et al., 2025; Shi et al., 2024) and physical understanding in VLMs, spanning from everyday scenes (Zheng et al., 2024; Chow et al., 2025a) to high-school physics questions (Wang et al., 2025) and Olympiad-level problems (Qiu et al., 2025; Wang et al., 2025), these efforts focus either on video generation or physical properties in static scenes, leaving underexplored whether VLMs can genuinely reason about physical transformations—where specific properties may or may not remain invariant.

To bridge this gap, we evaluate *conservation* in VLMs—the understanding that physical quantities remain invariant under transformation despite changes in appearance. Here, physical quantity refers to the measurable magnitude of objects along certain dimensions, while spatial transformation denotes the continuous process through which objects change in appearance or position. For example, an agent demonstrating conservation would recognize that pouring water into a differently shaped glass does not alter its volume, despite the change in visible form. Achieving conservation thus requires more than linguistic knowledge of quantity: it demands a systematic understanding that is both reversible and grounded in visual as well as conceptual representations. We introduce *ConservationBench*, a cognitively grounded benchmark for evaluating whether VLMs can reason about physical transformations. The benchmark consists of 192 video-based tasks across four core quanti-

^{*}Equal contribution ¹University of Michigan ²University of California San Diego ³University of California Berkeley ⁴Johns Hopkins University ⁵Emory University ⁶University of Toronto ⁷Brown University ⁸Auburn University ⁹Carnegie Mellon University. Correspondence to: Dezhi Luo <ihzedoul@umich.edu>, Yijiang Li <yijiangli@ucsd.edu>.

Task	Question	Conserving			Non-conserving		
Number	Is the number of coins in the upper row the same as in the lower row in the final image?						
Length	Is the length of the upper straw the same as the length of the lower in the final image?						
Size	Is the size of the playdough in the first image the same as in the final image?						
Volume	Is the amount of liquid in the left glass in the first image the same as in the right in the final image?						

Figure 1. Illustrative Tasks and Frame Selection Pipeline in *Conservation Bench*.

tative properties (number, length, volume, and size), each requiring models to judge whether a quantity is conserved despite visual transformations. To control for shortcut exploitation, we include 192 matched non-conserving controls where the target quantity changes while irrelevant features remain constant. We systematically vary frame extraction method, temporal resolution, and prompting strategy, yielding 60 conditions and 23,040 total trials.

Evaluating 112 VLMs, we find that models consistently fail to integrate temporal information to track conserved properties across dynamic scenes. High accuracy on conservation tasks is often driven by default heuristics, which reverse in non-conserving scenarios, revealing brittle, non-generalizable reasoning. Furthermore, prompting with cues encouraging transformation reasoning or providing higher temporal resolution does not help. These findings expose a fundamental limitation in current VLMs and underscore the need for more grounded, temporally-aware models capable of systematic physical inference.

2. Related Works

Evaluating VLMs. Early benchmarking efforts relied on single-task benchmarks such as VQA (Antol et al., 2015), OK-VQA (Marino et al., 2019), and OCR (Liu et al., 2023). However, with the emergence of VLMs that claim broader perceptual and reasoning abilities, evaluation has shifted toward holistic benchmarks such as MMMU (Yue et al., 2024), SEED-Bench (Li et al., 2024), and MMBench (Liu et al., 2024). A growing line of benchmarks focuses specifically on quantity understanding (Rane et al., 2024; Paiss et al., 2023; Rahmanzadehgervi et al., 2024; Yuksekogonul et al., 2022). These tasks typically assess a model’s ability to individuate and count discrete objects in static scenes. While useful, such evaluations largely reduce to surface-level enumeration and do not test whether models encode numerical invariance—invariance of quantity across transformations.

In contrast, our work examines whether VLMs go beyond perceptual counting to represent quantity as a conserved property.

Physical Understanding and Conservation. Insights from cognitive science underscore conservation as a critical benchmark for systematic physical reasoning. First proposed by Piaget, success on conservation tasks has long been viewed as evidence of emerging mental operations (Piaget & Inhelder, 1969). Developmental studies show that solving these tasks requires constructing transformation-invariant representations while suppressing misleading perceptual cues (Goldin-Meadow & Beilock, 2010; Houdé et al., 2011; Poirel et al., 2012). Behavioral and neurocognitive research further demonstrates that conservation performance depends on sensorimotor grounding and inhibitory control, highlighting the embodied nature of transformation understanding (Beilock & Goldin-Meadow, 2010; Lozada & Carro, 2016). Conservation also builds on more rudimentary abilities such as object permanence and individuation, revealed through studies exploiting the tunnel effect and violation-of-expectation paradigms (Burke, 1952; Flombaum & Scholl, 2006; Noles et al., 2005; Scholl, 2007), which themselves provide essential foundations for robust physical reasoning. In this light, conservation is widely recognized as a fundamental cognitive capacity for the higher-level physical reasoning needed to navigate dynamic, embodied environments (Fodor, 1975; Baillargeon & Carey, 2012; Barsalou, 2020; Luo et al., 2025b).

Recent studies have examined models’ abilities to reason about physical properties, causal interactions, and material dynamics (Chow et al., 2025a; Patel et al., 2022; Zheng et al., 2024; Li et al., 2025a). Growing evidence suggests that VLMs struggle with fundamental aspects of visual reasoning and physical understanding (Campbell et al., 2024; Gao et al., 2024b; Sun et al., 2024; 2025; Gao et al., 2025; Schulze Buschoff et al., 2025; Buschoff et al., 2025), with

some work exploring how modular frameworks or synthetic training data might address these limitations (Balazadeh et al., 2024; 2025; Luo et al., 2025b). However, these efforts largely emphasize outcome prediction or descriptive inference, without testing whether models recognize that certain properties remain invariant under transformation. In many cases, success appears to stem from outcome-based heuristics rather than structured mental operations (Newman et al., 2024; Isola et al., 2015). Consequently, it remains unclear whether current VLMs can genuinely integrate sequential evidence to track physical transformations while maintaining stable representations of underlying properties—a core cognitive capacity directly targeted by conservation tasks (Mitchell & Krakauer, 2023).

3. Experimental Design

3.1. Conservation Tasks

To systematically measure the conservation ability of VLMs—the understanding that specific physical properties remain invariant under transformations despite changes in appearance, we construct a suite of conservation tasks in the form of videos that visually depict physical transformations across four fundamental quantitative properties. We illustrate conservation tasks across each property in Figure 2, with full descriptions provided in Appendix B.

Although the four conservation types probe distinct physical properties, the tasks follow a unified structure: a transition from an initial to a final state mediated by an observable transformation. Each video begins with an initial state, proceeds through a continuous transformation (e.g., pouring, spreading, flattening), and ends with a new state where the surface appearance of the object of interest is altered. This design mirrors real-world scenarios where physical reasoning depends on integrating perceptual evidence across time.

Generalization across Task-irrelevant Features. To ensure the robustness and generalizability of the conclusions drawn from our benchmark, we systematically vary key visual parameters in each conservation task (Table 4). These parameters include object count, size, color, layout, container shape, and the direction of transformation. Each conservation property consists of 48 unique video instances of different configurations, resulting in a total of 192 videos. This controlled variation guarantees that the core conservation principle is preserved across a wide range of visual contexts, thus preventing models from relying on memorized templates or superficial cues.

Transformation-mandatory vs. -helpful. Notably, conservation tasks differ in how strongly they depend on observing the transformation. We classify them into two categories:

transformation-mandatory and *transformation-helpful*. In mandatory tasks (volume and size), witnessing the transformation is essential—for instance, in volume conservation, seeing the liquid poured is necessary, since the final height alone is insufficient for judging quantity. In helpful tasks (number and length), correct judgments can still be made from the initial and final states, as the relevant quantity remains visually accessible despite superficial changes. This distinction enables a more diagnostic evaluation: models that excel on helpful but not on mandatory tasks may rely on static cues rather than forming internal representations of the process.

To this end, we further curated a set of 96 tasks derived solely from the final frame of transformation-helpful tasks. Here, models are prompted to compare numbers and lengths directly based on simple counting and intuitive judgments of spatial extent. This design isolates pre-conceptual, rudimentary forms of quantitative assessment—such as item enumeration and perceptual matching—from the broader representational demands of transformation-based reasoning. By contrasting performance on these static tasks with temporal conservation trials, we can reveal how basic quantitative sensitivity relates to the more systematic representations of quantity that underlie conservation reasoning.

3.2. Non-conserving Tasks

A key limitation of applying conservation tasks to model evaluation is the uniformity of ground-truth labels: since all standard tasks involve quantity preservation, models can appear accurate simply by defaulting their responses to indicate invariance, due to biases from either visual contexts or linguistic patterns in the prompts, without genuinely reasoning about the physical transformation itself (Li et al., 2025b). To address this, we create non-conserving counterfactuals as a set of controlled experiments where the quantity of interest is explicitly altered during the transformation without changing the task-irrelevant features. That is to say, these manipulations are performed within the same environments, using identical object sets and visual contexts, thereby ensuring a controlled comparison. This design enables fine-grained assessment of model sensitivity to actual changes in quantity, rather than reliance on superficial heuristics or distributional priors. Details regarding control tasks across each property are available in Figure 2, with full descriptions provided in Appendix B. Following this design, we curated a control set in which each non-conserving control is paired with a conservation task under matched configurations, yielding an additional 192 videos.

3.3. Adaptation to Multi-frame Input

Temporal Resolution The ability to understand physical transformations critically depends on comprehending

dynamic processes over time. Unlike static snapshot reasoning, robust comprehension requires recognizing continuity across successive observations. Human perception benefits from high frame rates (e.g. ~ 30 -60 frames per second) that convey rich temporal information, while the architectural and computational limitations of VLMs restrict them to inferring such dynamics from discrete and often sparse inputs. To investigate the impact of temporal resolution on conservation understanding, we vary the number of frames extracted from each video:

- **3-frame condition:** Only three frames are provided—the first, the last, and one intermediate frame. This condition presents minimal temporal information while retaining just enough cues for humans to solve the task.
- **5-, 7-, and 9-frame condition:** More frames are sampled to offer moderate temporal granularity. This condition is designed to contrast qualitatively with the 3-frame condition by enabling multi-frame representations of the temporally continuous scene.
- **16-frame condition:** Sixteen frames are sampled to provide finer-grained temporal information, offering a more detailed depiction of the transformation process, contrasting quantitatively with the 8-frame condition.

All conditions include initial and final states. This design tests whether models can leverage higher temporal resolution to extract transformation-relevant information for conservation reasoning.

Sampling Strategy In studying physical transformations, the sequence and selection of visual inputs are crucial. This raises an important question: do different frame selection strategies influence the model’s understanding of dynamic scenes? Additionally, do humans and models rely on different criteria when identifying informative visual moments? To examine this, we implement and compare three frame extraction strategies, each reflecting distinct assumptions about what defines a “representative” moment in a physical event.

- **Uniform Sampling:** Frames are sampled uniformly across the timeline, serving as a baseline approach commonly used in prior work, based on the assumption that temporal regularity sufficiently represents informational diversity.
- **Human-based:** To obtain a baseline for human intuition in frame extraction, we recruited $N = 18$ annotators. Each annotator was randomly assigned a subset of the dataset and asked to manually select the intermediate frames that captured the essential stages of the transformation.

- **Model-based:** We adopt SEVILA (Yu et al., 2023) and leverage a BLIP-2-based Localizer to identify language-aware keyframes. Prompted with the same instruction assigned to humans (“extract the most complete set of frames that capture the entire process”), the Localizer module selects frames with high relevance scores, which are then passed to the Answerer module for inference. This method formalizes a strategy akin to semantic salience: choosing frames that are maximally informative given a specific query.

This design allows us to test whether different frame selection strategies affect model performance on physical transformation reasoning. We hypothesize that optimizing frame selection, rather than merely increasing frame quantity, leads to more effective representations of dynamic events. We detail our data curation process in Appendix A and prompting strategies in Appendix C, and provide example input in Appendix D.

Table 1. Overview of Multi-image Task Conditions and Evaluation Scale

Component	Count
<i>Core Dataset</i>	
Conservation Tasks	192
Non-conserving Control	192
Total Videos	384
<i>Multi-frame Conditions (Factorial)</i>	
Extraction Method	3
Frame Count	5
Prompting	4
Factorial Combinations	$3 \times 5 \times 4 = 60$
Total Evaluation Trials	$384 \times 60 = 23,040$

4. Experiments

4.1. Inference and Evaluation

Inference. We evaluate 112 VLMs spanning diverse model architectures, training data, and parameter scales, covering both mainstream commercial systems and advanced open-source models. To ensure fidelity, comparability, and reproducibility, we strictly adhere to reference configurations and implementations from the official codebases. Refer to Appendix E for further details.

Evaluation. To evaluate free-form outputs of VLMs on multiple-choice questions (MCQs), we follow the two-stage scoring method of Li et al. (2025a). In Stage 1, each VLM output is mapped to a unique choice from the provided options or labeled FAIL when no unambiguous mapping is possible. Mapping follows a hybrid strategy: deterministic template matching is applied first, and unresolved cases are adjudicated by an LLM-as-a-Judge constrained to the option set. Models exhibiting persistently high FAIL rates are ex-

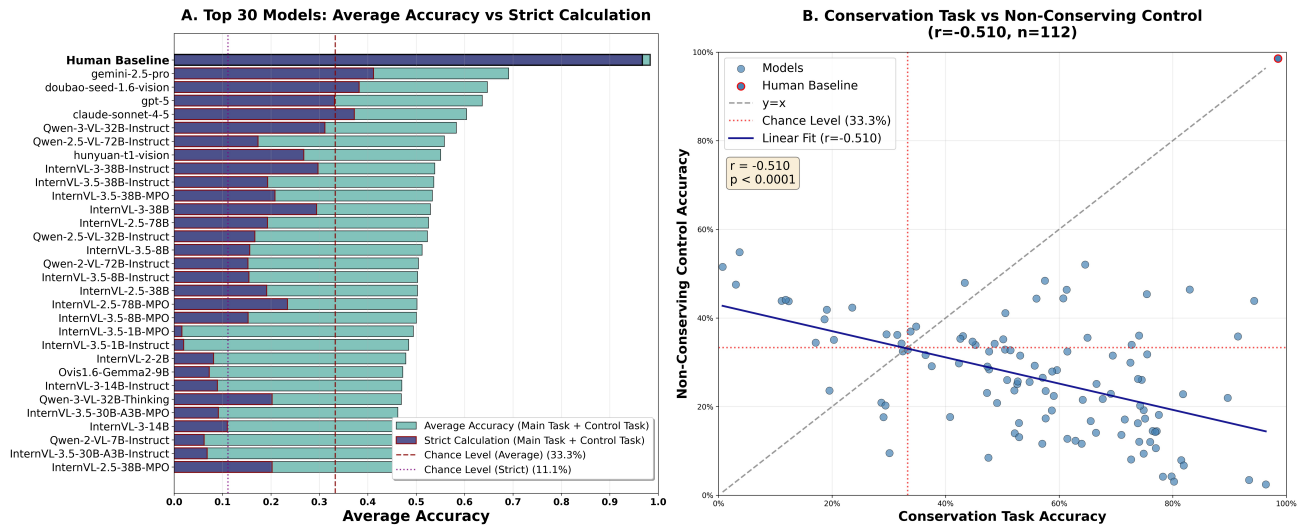


Figure 2. Overall Performance on *ConservationBench*. A. Accuracy averaged across conservation tasks and non-conserving control compared to strict pairwise calculation (Top 30 models; full results available in Appendix H; B. Performance on non-conserving control in relation to conservation tasks.

cluded from further analyses to avoid bias from nonsensical outputs. In Stage 2, the mapped option is compared against the ground-truth answer, with all FAILS scored as incorrect. Details are provided in Appendix F.

4.2. Human Baseline

Given the large number of questions and the cost of human annotation, we curated a representative subset by randomly selecting one out of every eight task configurations for each quantitative property, counterbalanced across conservation tasks and non-conserving controls. This resulted in a total of 864 questions. We hypothesize that reduced variation in task-irrelevant features is unlikely to compromise the benchmark’s validity or generalizability given the robustness of human reasoning. Participants received the same stimuli and three-choice questions as the VLMs, with the exception that they directly selected answers rather than requiring LLM judge parsing. The aggregated human accuracy reaches 98.35%, consistent with decades of developmental research showing that humans from late childhood reliably solve conservation tasks with near-perfect accuracy (Piaget, 1965; Houdé, 1997; Pezzulo et al., 2013; Viarouge et al., 2019). These results validate our benchmark design and its adaptation for evaluating VLMs. Detailed breakdown and comparison with models are highlighted in Appendix H.

4.3. Main Results

As shown in Figure 2A, model accuracy across 112 VLMs ranges from 20% to 69%, with most performing only marginally above the 33.3% chance level. In contrast, human participants exceed 98% accuracy (Section 4.2), high-

lighting a clear gap between VLMs and intuitive human reasoning. Collectively, these results reveal a core limitation: VLMs struggle to integrate temporal cues or track invariant properties through dynamic transformations, a key requirement for grounded physical reasoning. We report the performance of all models and human baseline in Appendix H.

Non-Conserving Control Reveal Systematic Bias By comparing model performance on non-conserving control tasks against conservation tasks, we observe a moderate negative correlation ($r = -0.510, n = 112$): models that perform better on conservation tasks tend to perform worse on the corresponding control tasks, and vice versa (Figure 2B). Most models cluster in the lower-right quadrant, exhibiting moderately high conservation accuracy (40–80%) but low non-conserving accuracy (10–40%), revealing a systematic bias toward quantity invariance regardless of actual transformation evidence. Only a small subset of models approaches balanced performance near the diagonal ($y = x$), while virtually none achieve high accuracy on both task types simultaneously. This pattern generalizes across four quantitative domains (see Appendix I for details). Crucially, this pattern reveals a diagnostic failure: models are not simply underperforming but exhibiting asymmetric reliance on default heuristics that systematically reverse across matched task conditions, demonstrating an inability to flexibly adjust reasoning based on transformation evidence.

We further validate this pattern using a *strict pairwise evaluation* across the full set matched conservation and non-conserving control tasks (Figure 2A; labeled in purple). In this analysis, a model is marked correct only if it answers

both tasks in a pair correctly—capturing whether it can jointly recognize quantity preservation and detect meaningful violations under matched visual conditions. We find that most models (82/112, 73.2%) perform well below chance, achieving strict accuracy rates under 10%. Only three top-performing models—GEMINI-2.5-PRO, DOUBAO-SEED-1.6-VISION, and CLAUDE-SONNET-4-5—exceed chance level (33.3%). This indicates that models are unable to reliably distinguish between conserving and non-conserving scenarios. The gap between average accuracy and strict evaluations suggests that models’ success are driven largely by bias toward quantity variance or invariance rather than genuine reasoning about physical transformations. This finding further supports the conclusion that models fail to internalize structured physical reasoning and instead rely on brittle default strategies for quantity assessment.

Dissociating Sources of Bias. To dissociate the source of bias—whether it arises from visual features or textual priors—we conducted two control experiments on 62 VLMs that support both image and text-only inputs. First, we reran the same experiments using fully white, content-free images while keeping all text input constant (**Empty Image Control**). Second, we removed visual input entirely, presenting only text prompts (**Text Control**). We used the 7-frame condition for all comparisons to enable direct pairwise evaluation. Model responses were evaluated as if they were answering standard conservation tasks. If performance were driven purely by visual cues, models should operate at chance when visual content is removed. Conversely, systematic deviations from chance would indicate reliance on textual biases—favoring either conservation (bias toward invariance) or non-conservation (bias toward perceptual change).

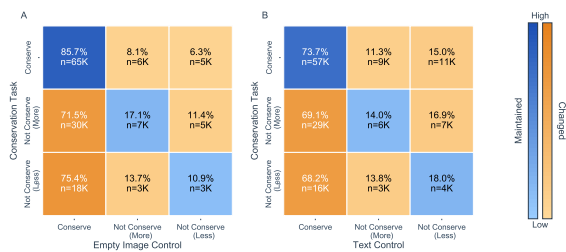


Figure 3. Response patterns under Empty Image and Text-only conditions compared to standard one. We report a distribution change in prediction between Empty Image and standard condition (A) to the left; Text-only control condition and standard condition (B) to the right.

Figure 3 reveals striking patterns in how models respond when visual information is degraded or removed. In the Empty Image Control (Panel A), when the actual conservation task required a "Conserve" answer, 85.7% of responses remained "Conserve" under empty images. Critically, when the actual task required "Not Conserve" answers, models

overwhelmingly switched to "Conserve" responses—71.5% for "More" scenarios and 75.4% for "Less" scenarios. The Text Control (Panel B) shows a similar but slightly attenuated pattern: 73.7% maintain "Conserve" answers, while 69.1% and 68.2% of non-conserving scenarios shift to "Conserve" responses. Further details regarding model-level trends in control condition responses compared to conservation task performance are provided in Appendix J.

These results reveal that textual priors strongly favor quantity invariance—a bias that is *correct* for conservation tasks but *incorrect* for non-conserving controls, explaining the inverse correlation we observe between conservation and non-conserving task performance. Notably, removing visual content while maintaining the visual modality (Empty Image) yields stronger conservation responses (85.7%) than removing the visual modality entirely (Text Control: 73.7%), suggesting that the presence of the visual channel amplifies textual biases even without meaningful visual information. Critically, however, models perform *worse* on actual conservation tasks with real visual content (average accuracy ~60%) than with empty images (85.7%), indicating that visual content actively interferes with the correct textual prior. Rather than enhancing transformation reasoning, visual information causes models to override their correct default bias with faulty visual processing. This demonstrates that the core deficit lies in visual transformation reasoning: models cannot reliably extract and integrate transformation-relevant information from sequential visual evidence, leading them to incorrectly reject quantity invariance even when visual content should confirm it. The combination of correct textual priors but impaired visual processing accounts for both the moderate success on conservation tasks and the systematic inverse failures on non-conserving controls.

4.4. Different Prompting Strategies, Frame Numbers, and Sampling Methods

We further analyzed model performance across three experimental factors—prompt type, frame count, and frame sampling method—evaluated separately for Number & Length versus Volume & Size conservation tasks. To properly account for the hierarchical structure of our data (multiple observations nested within 112 models), we employed repeated-measures ANOVA with models as the unit of analysis. For each model, we first averaged accuracy across the irrelevant experimental conditions (e.g., when testing frame number effects, we averaged across all prompt types and extraction methods), then conducted repeated-measures ANOVA to test main effects, followed by Bonferroni-corrected pairwise comparisons for significant factors. This approach accounts for the dependency structure in our data while avoiding inflated Type I error from treating non-independent observations as separate trials. We highlight the main conclusions below.

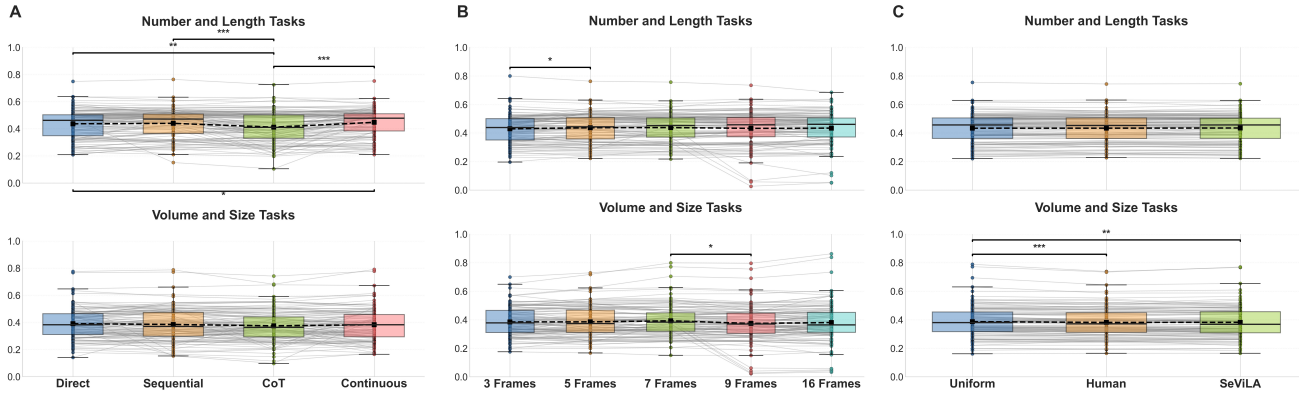


Figure 4. Model performance showing main effects by (A) prompt type, (B) number of frames, and (C) frame sampling method. Each panel averages across the other 2 factors from the full factorial design (4 prompts \times 5 frame counts \times 3 extraction methods).

Continuous cues aid performance, CoT makes it worse (Figure 4A). For Number & Length tasks, prompt type shows a highly significant main effect ($F(3, 333) = 18.28, p < 0.001$). Bonferroni-corrected pairwise comparisons reveal that CoT prompting performs significantly worse than all other prompt types: Continuous ($p < 0.001$), Sequential ($p < 0.001$), and Direct ($p = 0.0022$). Additionally, Continuous prompts—which explicitly frame transformations as continuous processes—significantly outperform Direct questions ($p = 0.0191$). These results indicate that conceptual cues emphasizing continuity can provide modest benefit for transformation-helpful tasks, while forcing step-by-step verbalization consistently impairs performance, likely by amplifying reliance on brittle heuristics. However, for Volume & Size tasks, prompt type shows no significant effect ($F(3, 333) = 2.00, p = 0.114$), suggesting that linguistic scaffolding provides no benefit when transformation reasoning demands are higher.

Temporal resolution shows no reliable benefit across task types (Figure 4B). For Number & Length tasks, frame count shows no significant main effect ($F(4, 444) = 0.98, p = 0.416$), indicating that additional frames do not reliably improve performance even when transformation cues are helpful. For Volume & Size tasks, frame count shows a modest significant effect ($F(4, 444) = 2.66, p = 0.032$), but Bonferroni-corrected pairwise comparisons reveal only one significant difference: 7 frames outperform 9 frames ($p_{\text{corrected}} = 0.0329$). This lack of consistent improvement with increased temporal information demonstrates that current VLMs are unable to effectively integrate sequential visual evidence for transformation reasoning. Additional frames do not enable models to track continuous physical changes, even when such tracking is essential for task success.

Frame extraction shows significant task-dependent effects (Figure 4C). For Number & Length tasks, extraction method shows no significant effect ($F(2, 222) = 1.36,$

$p = 0.258$), suggesting that different sampling methods perform comparably when transformation reasoning is helpful but not mandatory. However, for Volume & Size tasks, extraction method shows a highly significant effect ($F(2, 222) = 8.75, p = 0.0002$). Bonferroni-corrected pairwise comparisons reveal that uniform sampling significantly outperforms both human-selected ($p_{\text{corrected}} = 0.0006$) and SeViLA-selected frames ($p_{\text{corrected}} = 0.0014$), with no difference between the two curated methods ($p_{\text{corrected}} = 1.0$). These findings suggest that frame selection strategies interact weakly with task demands. For transformation-mandatory tasks (Volume & Size), curated frame selection even inadvertently emphasize misleading static features, suggesting that models are unable to utilize task-relevant biases for reasoning, further demonstrating the lack of ability to understand physical transformations.

4.5. Does Scaling of Model Size Help?

The advancement of LLMs has been closely tied to the empirical scaling law—predictable power-law improvements in performance with increased compute, parameters, and training data (Kaplan et al., 2020; Henighan et al., 2020; Zhai et al., 2022)—as well as emergence, the abrupt appearance of qualitatively new abilities as models grow larger (Wei et al., 2022; Aghajanyan et al., 2023; Bubeck et al., 2023; Berti et al., 2025). This raises a natural question: *Does the capacity to understand physical transformations and conservation similarly emerge with scale?*

To this end, we examine the performance v.s. model size (measured in log-scale parameters) across 112 VLMs, ranging from 1B to 76B parameters. We hold the frame number constant at 7 to control for potential confounding effects of multi-frame processing capacity. We find strikingly divergent patterns (Figure 7). For conservation tasks, model size exhibits virtually no predictive power ($R^2 = 0.019$). In contrast, non-conserving task accuracy exhibits a moderate positive relationship with model size ($R^2 = 0.239,$

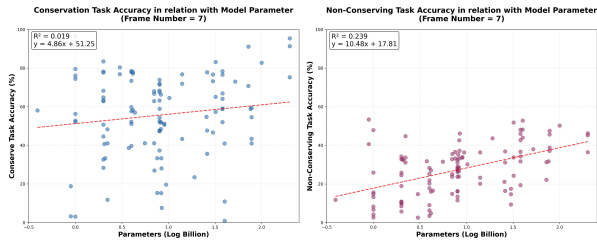


Figure 5. Conservation reasoning does not emerge with model scale. Model performance on (left) conservation tasks shows no relationship with parameter count ($R^2 = 0.019$), while (right) non-conserving task accuracy exhibits only modest scaling effects ($R^2 = 0.239$), both evaluated at 7-frame condition across 112 VLMs.

$y = 10.48x + 17.81$), indicating that larger models tend to do better on non-conserving controls. However, even this relationship accounts for less than 24% of the variance, with substantial scatter persisting across all model scales. These results demonstrate that conservation reasoning emerges only at a small scale in current VLMs.

5. Discussions

We introduce a cognitively grounded benchmark evaluating whether VLMs can reason about physical transformations through conservation tasks and non-conserving controls. Our findings reveal that current models consistently fail to integrate sequential visual evidence to maintain transformation-invariant representations of physical properties across dynamic scenes. Control experiments reveal that models possess strong textual priors favoring quantity invariance yet perform worse with actual visual content, revealing reliance on brittle heuristics. Neither increased temporal resolution, targeted prompting, nor human-curated frame sampling induces robust transformation reasoning. These results expose a fundamental deficit in structured physical understanding and highlight critical challenges for developing grounded AI systems capable of systematic inference in dynamic environments. Beyond documenting these failures, our benchmark provides an enduring diagnostic test as the field advances. The tasks curated in this study can serve as sanity checks for foundation models’ transformation reasoning, particularly as models achieve breakthroughs on high-level physical reasoning benchmarks while robustness challenges persist.

The failures documented in this work have direct implications for understanding VLMs’ capacity for physical reasoning and multi-frame understanding more broadly. Conservation reflects a foundational cognitive substrate that scaffolds higher-level physical reasoning in humans. The failure modes exposed here resonate with recent work arguing that without such core representations, higher-level abilities remain brittle and fail to generalize beyond curated

benchmarks. Models lacking transformation-invariant reasoning about basic quantities pose risks for robust physical understanding in complex, real-world scenarios (Li et al., 2025a; Cai et al., 2025). Moreover, our results suggest that limitations in encoding and processing sequential visual-spatial information likely constitute a primary bottleneck for transformation reasoning. This speaks to broader concerns regarding reliance on coarse-grained visual encodings in VLMs, which may be mechanistically unsuitable for conducting structured physical reasoning (Zhang et al., 2024a; Luo et al., 2025a; Fu et al., 2025). While our behavioral findings do not establish the precise architectural causes, we highlight the need for mechanistic investigations to identify the specific representational constraints prevent current models from constructing transformation-invariant object representations.

6. Conclusion and Limitation

We introduce a comprehensive benchmark on physically grounded inference property *conservation*, the principle that physical quantities remain invariant under transformations despite appearance changes. We show that current VLMs consistently fail to maintain transformation-invariant representations of physical properties across dynamic scenes. These failures indicate fundamental deficits in systematic physical reasoning, posing risks for tasks such as embodied AI. Our benchmark provides an enduring diagnostic test for transformation reasoning as the field advances.

We acknowledge several limitations in our study. First, our evaluation focuses on conservation tasks across four quantitative properties under controlled laboratory conditions. While targeting foundational cognitive capacities, more complex scenarios involving occlusions, deformable objects, noisy observations, and ambiguous transformations are planned for future work. Second, our study is primarily behavioral, documenting failure modes without establishing precise mechanistic causes. While we hypothesize that coarse-grained visual encodings prevent transformation-invariant representations, mechanistic interpretability studies to validate these claims are planned. Finally, our evaluation focuses on perceptual judgment rather than goal-directed applications. Whether conservation deficits impair downstream tasks such as planning, tool use, or robotic manipulation remains for future investigation.

Acknowledgments

This work was supported by a MiraclePlus Compute Grant to Growing AI Like A Child (<https://growing-ai-like-a-child.github.io/>).

References

- Aghajanyan, A., Yu, L., Conneau, A., Hsu, W.-N., Hambardzumyan, K., Zhang, S., Roller, S., Goyal, N., Levy, O., and Zettlemoyer, L. Scaling laws for generative mixed-modal language models. In *International Conference on Machine Learning*, pp. 265–279. PMLR, 2023.
- Alayrac, J.-B., Donahue, J., Luc, P., Miech, A., Barr, I., Hasson, Y., Lenc, K., Mensch, A., Millican, K., Reynolds, M., et al. Flamingo: a visual language model for few-shot learning. *Advances in neural information processing systems*, 35:23716–23736, 2022.
- Allen, K. R., Smith, K. A., and Tenenbaum, J. B. Rapid trial-and-error learning with simulation supports flexible tool use and physical reasoning. *Proceedings of the National Academy of Sciences*, 117(47):29302–29310, 2020.
- Antol, S., Agrawal, A., Lu, J., Mitchell, M., Batra, D., Zitnick, C. L., and Parikh, D. Vqa: Visual question answering. In *Proceedings of the IEEE international conference on computer vision*, pp. 2425–2433, 2015.
- Baillargeon, R. Representing the existence and the location of hidden objects: Object permanence in 6-and 8-month-old infants. *Cognition*, 23(1):21–41, 1986.
- Baillargeon, R. Young infants’ reasoning about the physical and spatial properties of a hidden object. *Cognitive development*, 2(3):179–200, 1987.
- Baillargeon, R. and Carey, S. Core cognition and beyond: The acquisition of physical and numerical knowledge. *Early childhood development and later outcome*, 1, 2012.
- Baillargeon, R., Spelke, E. S., and Wasserman, S. Object permanence in five-month-old infants. *Cognition*, 20(3):191–208, 1985.
- Baillargeon, R., Graber, M., Devos, J., and Black, J. Why do young infants fail to search for hidden objects? *Cognition*, 36(3):255–284, 1990.
- Balazadeh, V., Ataei, M., Cheong, H., Hosein Khasahmadi, A., and Krishnan, R. G. Synthetic vision: Training vision-language models to understand physics. *arXiv e-prints*, pp. arXiv-2412, 2024.
- Balazadeh, V., Ataei, M., Cheong, H., Khasahmadi, A. H., and Krishnan, R. G. Physics context builders: A modular framework for physical reasoning in vision-language models. In *Proceedings of the IEEE/CVF International Conference on Computer Vision*, pp. 7318–7328, 2025.
- Barsalou, L. W. Challenges and opportunities for grounding cognition. *Journal of Cognition*, 3(1), 2020.
- Bear, D. M., Wang, E., Mrowca, D., Binder, F. J., Tung, H.-Y. F., Pramod, R., Holdaway, C., Tao, S., Smith, K., Sun, F.-Y., et al. Physion: Evaluating physical prediction from vision in humans and machines. *arXiv preprint arXiv:2106.08261*, 2021.
- Beilock, S. and Goldin-Meadow, S. Gesture changes thought by grounding it in action. *Psychological Science*, 21(11):1605–1610, 2010.
- Berti, L., Giorgi, F., and Kasneci, G. Emergent abilities in large language models: A survey. *arXiv preprint arXiv:2503.05788*, 2025.
- Brohan, A., Brown, N., Carbajal, J., Chebotar, Y., Chen, X., Choremanski, K., Ding, T., Driess, D., Dubey, A., Finn, C., Florence, P., Fu, C., Arenas, M. G., Gopalakrishnan, K., Han, K., Hausman, K., Herzog, A., Hsu, J., Ichter, B., Irpan, A., Joshi, N., Julian, R., Kalashnikov, D., Kuang, Y., Leal, I., Lee, L., Lee, T.-W. E., Levine, S., Lu, Y., Michalewski, H., Mordatch, I., Pertsch, K., Rao, K., Reymann, K., Ryoo, M., Salazar, G., Sanketi, P., Sermanet, P., Singh, J., Singh, A., Soricut, R., Tran, H., Vanhoucke, V., Vuong, Q., Wahid, A., Welker, S., Wohlhart, P., Wu, J., Xia, F., Xiao, T., Xu, P., Xu, S., Yu, T., and Zitkovich, B. Rt-2: Vision-language-action models transfer web knowledge to robotic control, 2023. URL <https://arxiv.org/abs/2307.15818>.
- Bubeck, S., Chadrasekaran, V., Eldan, R., Gehrke, J., Horvitz, E., Kamar, E., Lee, P., Lee, Y. T., Li, Y., Lundberg, S., et al. Sparks of artificial general intelligence: Early experiments with gpt-4, 2023.
- Burke, L. On the tunnel effect. *Quarterly Journal of Experimental Psychology*, 4(3):121–138, 1952.
- Buschhoff, L. M. S., Voudouris, K., Akata, E., Bethge, M., Tenenbaum, J. B., and Schulz, E. Testing the limits of fine-tuning to improve reasoning in vision language models. *arXiv preprint arXiv:2502.15678*, 2025.
- Cai, Z., Wang, Y., Sun, Q., Wang, R., Gu, C., Yin, W., Lin, Z., Yang, Z., Wei, C., Qian, O., et al. Holistic evaluation of multimodal llms on spatial intelligence. *arXiv preprint arXiv:2508.13142*, 2025.
- Campbell, D., Rane, S., Giallanza, T., De Sabbata, C. N., Ghods, K., Joshi, A., Ku, A., Frankland, S., Griffiths, T., Cohen, J. D., et al. Understanding the limits of vision language models through the lens of the binding problem. *Advances in Neural Information Processing Systems*, 37:113436–113460, 2024.
- Chen, Z., Wang, W., Cao, Y., Liu, Y., Gao, Z., Cui, E., Zhu, J., Ye, S., Tian, H., Liu, Z., Gu, L., Wang, X., Li, Q., Ren, Y., Chen, Z., Luo, J., Wang, J., Jiang, T., Wang, B.,

- He, C., Shi, B., Zhang, X., Lv, H., Wang, Y., Shao, W., Chu, P., Tu, Z., He, T., Wu, Z., Deng, H., Ge, J., Chen, K., Zhang, K., Wang, L., Dou, M., Lu, L., Zhu, X., Lu, T., Lin, D., Qiao, Y., Dai, J., and Wang, W. Expanding performance boundaries of open-source multimodal models with model, data, and test-time scaling, 2025. URL <https://arxiv.org/abs/2412.05271>.
- Cheng, K., Li, Y., Xu, F., Zhang, J., Zhou, H., and Liu, Y. Vision-language models can self-improve reasoning via reflection. *arXiv preprint arXiv:2411.00855*, 2024a.
- Cheng, Z., Leng, S., Zhang, H., Xin, Y., Li, X., Chen, G., Zhu, Y., Zhang, W., Luo, Z., Zhao, D., and Bing, L. Videollama 2: Advancing spatial-temporal modeling and audio understanding in video-llms, 2024b. URL <https://arxiv.org/abs/2406.07476>.
- Chow, W., Mao, J., Li, B., Seita, D., Guizilini, V., and Wang, Y. Physbench: Benchmarking and enhancing vision-language models for physical world understanding. *arXiv preprint arXiv:2501.16411*, 2025a.
- Chow, W., Mao, J., Li, B., Seita, D., Guizilini, V., and Wang, Y. Physbench: Benchmarking and enhancing vision-language models for physical world understanding, 2025b. URL <https://arxiv.org/abs/2501.16411>.
- Driess, D., Xia, F., Sajjadi, M. S. M., Lynch, C., Chowdhery, A., Ichter, B., Wahid, A., Tompson, J., Vuong, Q., Yu, T., Huang, W., Chebotar, Y., Sermanet, P., Duckworth, D., Levine, S., Vanhoucke, V., Hausman, K., Toussaint, M., Greff, K., Zeng, A., Mordatch, I., and Florence, P. Palm-e: An embodied multimodal language model, 2023. URL <https://arxiv.org/abs/2303.03378>.
- Flombaum, J. I. and Scholl, B. J. A temporal same-object advantage in the tunnel effect: facilitated change detection for persisting objects. *Journal of Experimental Psychology: Human Perception and Performance*, 32(4):840, 2006.
- Fodor, J. A. *The Language of Thought*. MIT Press, 1975.
- Fu, S., Bonnen, T., Guillory, D., and Darrell, T. Hidden in plain sight: Vlms overlook their visual representations. *arXiv preprint arXiv:2506.08008*, 2025.
- Gao, J., Sarkar, B., Xia, F., Xiao, T., Wu, J., Ichter, B., Majumdar, A., and Sadigh, D. Physically grounded vision-language models for robotic manipulation, 2024a. URL <https://arxiv.org/abs/2309.02561>.
- Gao, Q., Li, Y., Lyu, H., Sun, H., Luo, D., and Deng, H. Vision language models see what you want but not what you see. *arXiv preprint arXiv:2410.00324*, 2024b.
- Gao, Q., Pi, X., Liu, K., Chen, J., Yang, R., Huang, X., Fang, X., Sun, L., Kishore, G., Ai, B., et al. Do vision-language models have internal world models? towards an atomic evaluation. *arXiv preprint arXiv:2506.21876*, 2025.
- Goldin-Meadow, S. and Beilock, S. Action’s influence on thought: the case of gesture. *Perspectives on psychological science : a journal of the Association for Psychological Science*, 5(6):664–674, 2010.
- Gredebäck, G. and von Hofsten, C. Infants’ evolving representations of object motion during occlusion: A longitudinal study of 6- to 12-month-old infants. *Infancy*, 6(2): 165–184, 2004. doi: 10.1207/s15327078in0602_2.
- Henighan, T., Kaplan, J., Katz, M., Chen, M., Hesse, C., Jackson, J., Jun, H., Brown, T. B., Dhariwal, P., Gray, S., et al. Scaling laws for autoregressive generative modeling. *arXiv preprint arXiv:2010.14701*, 2020.
- Houdé, O. Numerical development: From the infant to the child. *Cognitive Development*, 12(3):373–391, 1997.
- Houdé, O., Pineau, A., Leroux, G., Poirel, N., Perchey, G., Lanoë, C., Lubin, A., Turbelin, M.-R., Rossi, S., Simon, G., Delcroix, N., Lambertson, F., Vigneau, M., Wisniewski, G., Vicet, J.-R., and Mazoyer, B. Functional magnetic resonance imaging study of piaget’s conservation-of-number task in preschool and school-age children: a neo-piagetian approach. *Journal of experimental child psychology*, 110(3):332–346, 2011.
- Isola, P., Lim, J. J., and Adelson, E. H. Discovering states and transformations in image collections. In *Proceedings of the IEEE conference on computer vision and pattern recognition*, pp. 1383–1391, 2015.
- Jiang, Y., Wang, Y., Zhao, R., Parag, T., Chen, Z., Liao, Z., and Unnikrishnan, J. Videop2r: Video understanding from perception to reasoning. *arXiv preprint arXiv:2511.11113*, 2025.
- Kaplan, J., McCandlish, S., Henighan, T., Brown, T. B., Chess, B., Child, R., Gray, S., Radford, A., Wu, J., and Amodei, D. Scaling laws for neural language models. *arXiv preprint arXiv:2001.08361*, 2020.
- Li, B., Ge, Y., Ge, Y., Wang, G., Wang, R., Zhang, R., and Shan, Y. Seed-bench: Benchmarking multimodal large language models. In *Proceedings of the IEEE/CVF Conference on Computer Vision and Pattern Recognition*, pp. 13299–13308, 2024.
- Li, J., Li, D., Savarese, S., and Hoi, S. Blip-2: Bootstrapping language-image pre-training with frozen image encoders and large language models. *CONFERENCE*, 2023.

- Li, Y., Gao, Q., Zhao, T., Wang, B., Sun, H., Lyu, H., Hawkins, R. D., Vasconcelos, N., Golan, T., Luo, D., and Deng, H. Core knowledge deficits in multi-modal language models. *arXiv preprint arXiv:2410.10855*, 2025a.
- Li, Y., Wang, B., Zhao, T., Gao, Q., Deng, H., and Luo, D. Evaluating multi-modal language models through concept hacking. In *Workshop on Spurious Correlation and Shortcut Learning: Foundations and Solutions*, 2025b.
- Liu, D., Zhang, J., Dinh, A.-D., Park, E., Zhang, S., Mian, A., Shah, M., and Xu, C. Generative physical ai in vision: A survey, 2025. URL <https://arxiv.org/abs/2501.10928>.
- Liu, Y., Li, Z., Yang, B., Li, C., Yin, X., Liu, C.-l., Jin, L., and Bai, X. On the hidden mystery of ocr in large multimodal models. *arXiv preprint arXiv:2305.07895*, 2023.
- Liu, Y., Duan, H., Zhang, Y., Li, B., Zhang, S., Zhao, W., Yuan, Y., Wang, J., He, C., Liu, Z., et al. Mmbench: Is your multi-modal model an all-around player? In *European conference on computer vision*, pp. 216–233. Springer, 2024.
- Lozada, M. and Carro, N. Embodied action improves cognition in children: Evidence from a study based on piagetian conservation tasks. *Frontiers in psychology*, 7(393), 2016.
- Luo, D., Gao, Q., and Deng, H. Rethinking the simulation vs. rendering dichotomy: No free lunch in spatial world modelling. *arXiv preprint arXiv:2510.20835*, 2025a.
- Luo, D., Li, Y., and Deng, H. The philosophical foundations of growing ai like a child. *arXiv preprint arXiv:2502.10742*, 2025b.
- Marino, K., Rastegari, M., Farhadi, A., and Mottaghi, R. Ok-vqa: A visual question answering benchmark requiring external knowledge. In *Proceedings of the IEEE/cvf conference on computer vision and pattern recognition*, pp. 3195–3204, 2019.
- Meng, F., Liao, J., Tan, X., Shao, W., Lu, Q., Zhang, K., Cheng, Y., Li, D., Qiao, Y., and Luo, P. Towards world simulator: Crafting physical commonsense-based benchmark for video generation, 2024. URL <https://arxiv.org/abs/2410.05363>.
- Mitchell, M. and Krakauer, D. C. The debate over understanding in ai’s large language models. *Proceedings of the National Academy of Sciences*, 120(13):e2215907120, 2023.
- Motamed, S., Culp, L., Swersky, K., Jaini, P., and Geirhos, R. Do generative video models understand physical principles?, 2025. URL <https://arxiv.org/abs/2501.09038>.
- Nasiriany, S., Xia, F., Yu, W., Xiao, T., Liang, J., Dasgupta, I., Xie, A., Driess, D., Wahid, A., Xu, Z., Vuong, Q., Zhang, T., Lee, T.-W. E., Lee, K.-H., Xu, P., Kirmani, S., Zhu, Y., Zeng, A., Hausman, K., Heess, N., Finn, C., Levine, S., and Ichter, B. Pivot: Iterative visual prompting elicits actionable knowledge for vlms, 2024. URL <https://arxiv.org/abs/2402.07872>.
- Newman, K., Wang, S., Zang, Y., Heffren, D., and Sun, C. Do pre-trained vision-language models encode object states? *arXiv preprint arXiv:2409.10488*, 2024.
- Noles, N. S., Scholl, B. J., and Mitroff, S. R. The persistence of object file representations. *Perception & Psychophysics*, 67(2):324–334, 2005.
- Paiss, R., Ephrat, A., Tov, O., Zada, S., Mosseri, I., Irani, M., and Dekel, T. Teaching clip to count to ten. In *Proceedings of the IEEE/CVF International Conference on Computer Vision*, pp. 3170–3180, 2023.
- Park, J. S., Bhagavatula, C., Mottaghi, R., Farhadi, A., and Choi, Y. Visualcomet: Reasoning about the dynamic context of a still image, 2020. URL <https://arxiv.org/abs/2004.10796>.
- Patel, M., Gokhale, T., Baral, C., and Yang, Y. Crippvqa: Counterfactual reasoning about implicit physical properties via video question answering. *arXiv preprint arXiv:2211.03779*, 2022.
- Pezzulo, G., Barsalou, L. W., Cangelosi, A., Fischer, M. H., McRae, K., and Spivey, M. J. Computational grounded cognition: a new alliance between grounded cognition and computational modeling. *Frontiers in psychology*, 3: 612, 2013.
- Piaget, J. *The Psychology of Intelligence*. Harcourt, Brace, 1950.
- Piaget, J. *The Origins of Intelligence in Children*. International Universities Press, 1952.
- Piaget, J. *The Child’s Conception of Number*. W.W. Norton and Company, 1965.
- Piaget, J. and Inhelder, B. *The Psychology of the Child*. Basic Books, New York, 1969.
- Piloto, L. S., Weinstein, A., Battaglia, P., and Botvinick, M. Intuitive physics learning in a deep-learning model inspired by developmental psychology. *Nature human behaviour*, 6(9):1257–1267, 2022.

- Poirel, N., Borst, G., Simon, G., Rossi, S., Cassotti, M., Pineau, A., and Houdé, O. Number conservation is related to children’s prefrontal inhibitory control: an fmri study of a piagetian task. *PLoS one*, 7(7):e40802, 2012.
- Qiu, S., Guo, S., Song, Z.-Y., Sun, Y., Cai, Z., Wei, J., Luo, T., Yin, Y., Zhang, H., Hu, Y., et al. Phybench: Holistic evaluation of physical perception and reasoning in large language models. *arXiv preprint arXiv:2504.16074*, 2025.
- Radford, A., Kim, J. W., Hallacy, C., Ramesh, A., Goh, G., Agarwal, S., Sastry, G., Askell, A., Mishkin, P., Clark, J., Krueger, G., and Sutskever, I. Learning transferable visual models from natural language supervision. *arXiv preprint arXiv: 2103.00020*, 2021.
- Rahmanzadehgervi, P., Bolton, L., Taesiri, M. R., and Nguyen, A. T. Vision language models are blind. *arXiv preprint arXiv:2407.06581*, 2024.
- Rane, S., Ku, A., Baldrige, J., Tenney, I., Griffiths, T., and Kim, B. Can generative multimodal models count to ten? *Proceeding of the Annual Meeting of the Cognitive Science Society*, 46:1235–1241, 2024.
- Scholl, B. J. Object persistence in philosophy and psychology. *Mind & Language*, 22(5):563–591, 2007.
- Schulze Buschoff, L. M., Akata, E., Bethge, M., and Schulz, E. Visual cognition in multimodal large language models. *Nature Machine Intelligence*, 7(1):96–106, 2025.
- Shi, X., Huang, Z., Wang, F.-Y., Bian, W., Li, D., Zhang, Y., Zhang, M., Cheung, K. C., See, S., Qin, H., Dai, J., and Li, H. Motion-i2v: Consistent and controllable image-to-video generation with explicit motion modeling, 2024. URL <https://arxiv.org/abs/2401.15977>.
- Spelke, E. S., Breinlinger, K., Macomber, J., and Jacobson, K. Origins of knowledge. *Psychological review*, 99(4): 605, 1992.
- Spelke, E. S., Katz, G., Purcell, S. E., Ehrlich, S. M., and Breinlinger, K. Early knowledge of object motion: Continuity and inertia. *Cognition*, 51(2):131–176, 1994.
- Spelke, E. S., Kestenbaum, R., Simons, D. J., and Wein, D. Spatiotemporal continuity, smoothness of motion and object identity in infancy. *British journal of developmental psychology*, 13(2):113–142, 1995.
- Sun, H., Gao, Q., Lyu, H., Luo, D., Li, Y., and Deng, H. Probing mechanical reasoning in large vision language models. *arXiv preprint arXiv:2410.00318*, 2024.
- Sun, H., Yu, S., Li, Y., Gao, Q., Lyu, H., Deng, H., and Luo, D. Probing perceptual constancy in large vision language models. *arXiv preprint arXiv:2502.10273*, 2025.
- Team, G., Kamath, A., Ferret, J., Pathak, S., Vieillard, N., Merhej, R., Perrin, S., Matejovicova, T., Ramé, A., Rivière, M., Rouillard, L., Mesnard, T., Cideron, G., bastien Grill, J., Ramos, S., Yvinec, E., Casbon, M., Pot, E., Penchev, I., Liu, G., Visin, F., Kenealy, K., Beyer, L., Zhai, X., Tsitsulin, A., Busa-Fekete, R., Feng, A., Sachdeva, N., Coleman, B., Gao, Y., Mustafa, B., Barr, I., Parisotto, E., Tian, D., Eyal, M., Cherry, C., Peter, J.-T., Sinopalnikov, D., Bhupatiraju, S., Agarwal, R., Kazemi, M., Malkin, D., Kumar, R., Vilar, D., Brusilovsky, I., Luo, J., Steiner, A., Friesen, A., Sharma, A., Sharma, A., Gilady, A. M., Goedeckemeyer, A., Saade, A., Feng, A., Kolesnikov, A., Bendebury, A., Abdagic, A., Vadi, A., György, A., Pinto, A. S., Das, A., Bapna, A., Miech, A., Yang, A., Paterson, A., Shenoy, A., Chakrabarti, A., Piot, B., Wu, B., Shahriari, B., Petrini, B., Chen, C., Lan, C. L., Choquette-Choo, C. A., Carey, C., Brick, C., Deutsch, D., Eisenbud, D., Cattle, D., Cheng, D., Paparas, D., Sreepathihalli, D. S., Reid, D., Tran, D., Zelle, D., Noland, E., Huizenga, E., Kharitonov, E., Liu, F., Amirkhanyan, G., Cameron, G., Hashemi, H., Klimczak-Plucińska, H., Singh, H., Mehta, H., Lehri, H. T., Hazimeh, H., Ballantyne, I., Szpektor, I., Nardini, I., Pouget-Abadie, J., Chan, J., Stanton, J., Wieting, J., Lai, J., Orbay, J., Fernandez, J., Newlan, J., yeong Ji, J., Singh, J., Black, K., Yu, K., Hui, K., Vodrahalli, K., Greff, K., Qiu, L., Valentine, M., Coelho, M., Ritter, M., Hoffman, M., Watson, M., Chaturvedi, M., Moynihan, M., Ma, M., Babar, N., Noy, N., Byrd, N., Roy, N., Momchev, N., Chauhan, N., Sachdeva, N., Bunyan, O., Botarda, P., Caron, P., Rubenstein, P. K., Culliton, P., Schmid, P., Sessa, P. G., Xu, P., Stanczyk, P., Tafti, P., Shivanna, R., Wu, R., Pan, R., Rokni, R., Willoughby, R., Vallu, R., Mullins, R., Jerome, S., Smoot, S., Giringin, S., Iqbal, S., Reddy, S., Sheth, S., Pöder, S., Bhatnagar, S., Panyam, S. R., Eiger, S., Zhang, S., Liu, T., Yacovone, T., Liechty, T., Kalra, U., Evcı, U., Misra, V., Roseberry, V., Feinberg, V., Kolesnikov, V., Han, W., Kwon, W., Chen, X., Chow, Y., Zhu, Y., Wei, Z., Egyed, Z., Cotruta, V., Giang, M., Kirk, P., Rao, A., Black, K., Babar, N., Lo, J., Moreira, E., Martins, L. G., Sanseviero, O., Gonzalez, L., Gleicher, Z., Warkentin, T., Mirrokni, V., Senter, E., Collins, E., Barral, J., Ghahramani, Z., Hadsell, R., Matias, Y., Sculley, D., Petrov, S., Fiedel, N., Shazeer, N., Vinyals, O., Dean, J., Hassabis, D., Kavukcuoglu, K., Farabet, C., Buchatskaya, E., Alayrac, J.-B., Anil, R., Dmitry, Lepikhin, Borgeaud, S., Bachem, O., Joulin, A., Andreev, A., Hardin, C., Dadashi, R., and Hussenot, L. Gemma 3 technical report, 2025. URL <https://arxiv.org/abs/2503.19786>.
- Viarouge, A., Houdé, O., and Borst, G. The progressive 6-year-old conserver: Numerical saliency and sensitivity as core mechanisms of numerical abstraction in a piaget-like

- estimation task. *Cognition*, 190:137–142, 2019.
- Wang, L., Su, E., Liu, J., Li, P., Xia, P., Xiao, J., Zhang, W., Dai, X., Chen, X., Meng, Y., et al. Physunibench: An undergraduate-level physics reasoning benchmark for multimodal models. *arXiv preprint arXiv:2506.17667*, 2025.
- Wang, P., Bai, S., Tan, S., Wang, S., Fan, Z., Bai, J., Chen, K., Liu, X., Wang, J., Ge, W., Fan, Y., Dang, K., Du, M., Ren, X., Men, R., Liu, D., Zhou, C., Zhou, J., and Lin, J. Qwen2-vl: Enhancing vision-language model’s perception of the world at any resolution, 2024. URL <https://arxiv.org/abs/2409.12191>.
- Wei, J., Tay, Y., Bommasani, R., Raffel, C., Zoph, B., Borgeaud, S., Yogatama, D., Bosma, M., Zhou, D., Metzler, D., et al. Emergent abilities of large language models. *arXiv preprint arXiv:2206.07682*, 2022.
- Xu, G., Jin, P., Hao, L., Song, Y., Sun, L., and Yuan, L. Llava-o1: Let vision language models reason step-by-step. *arXiv preprint arXiv:2411.10440*, 2024.
- Yang, X., Li, B., Zhang, Y., Yin, Z., Bai, L., Ma, L., Wang, Z., Cai, J., Wong, T.-T., Lu, H., and Jia, X. Vlipp: Towards physically plausible video generation with vision and language informed physical prior, 2025. URL <https://arxiv.org/abs/2503.23368>.
- Yu, S., Cho, J., Yadav, P., and Bansal, M. Self-chained image-language model for video localization and question answering. *Advances in Neural Information Processing Systems*, 36:76749–76771, 2023.
- Yue, X., Ni, Y., Zhang, K., Zheng, T., Liu, R., Zhang, G., Stevens, S., Jiang, D., Ren, W., Sun, Y., et al. Mmmu: A massive multi-discipline multimodal understanding and reasoning benchmark for expert agi. In *Proceedings of the IEEE/CVF Conference on Computer Vision and Pattern Recognition*, pp. 9556–9567, 2024.
- Yuksekgonul, M., Bianchi, F., Kalluri, P., Jurafsky, D., and Zou, J. When and why vision-language models behave like bags-of-words, and what to do about it? *arXiv preprint arXiv:2210.01936*, 2022.
- Zellers, R., Bisk, Y., Farhadi, A., and Choi, Y. From recognition to cognition: Visual commonsense reasoning, 2019. URL <https://arxiv.org/abs/1811.10830>.
- Zhai, X., Kolesnikov, A., Houlsby, N., and Beyer, L. Scaling vision transformers. In *Proceedings of the IEEE/CVF conference on computer vision and pattern recognition*, pp. 12104–12113, 2022.
- Zhang, J., Hu, J., Khayatkhoei, M., Iliovski, F., and Sun, M. Exploring perceptual limitation of multimodal large language models. *arXiv preprint arXiv:2402.07384*, 2024a.
- Zhang, R., Zhang, B., Li, Y., Zhang, H., Sun, Z., Gan, Z., Yang, Y., Pang, R., and Yang, Y. Improve vision language model chain-of-thought reasoning. *arXiv preprint arXiv:2410.16198*, 2024b.
- Zhang, Y., Wu, J., Li, W., Li, B., Ma, Z., Liu, Z., and Li, C. Video instruction tuning with synthetic data, 2024c. URL <https://arxiv.org/abs/2410.02713>.
- Zheng, Z., Yan, X., Chen, Z., Wang, J., Lim, Q. Z. E., Tenenbaum, J. B., and Gan, C. Contphy: Continuum physical concept learning and reasoning from videos. *arXiv preprint arXiv:2402.06119*, 2024.

A. Data Curation

Curation and Quality Control. *ConservationBench* was curated by three annotators with college-level training in cognitive science or computer science. Each video underwent two independent cross-review passes; items failing to meet design criteria were removed or revised.

Data Acquisition. All videos were captured under standardized recording conditions using a fixed camera setup, with consistent lighting and background held constant within each property category. Each transformation was carefully scripted to ensure visual clarity, reproducibility, and minimal ambiguity.

Design Principles. To ensure conceptual integrity and interdisciplinary rigor, we adopt three design criteria for each item: (i) *Discriminativeness*—tasks are constructed such that models lacking the targeted knowledge are systematically driven toward incorrect responses; (ii) *Minimal confounding*—instances are designed to minimize reliance on ancillary skills (e.g., object recognition); and (iii) *Minimal textual shortcuts*—tasks cannot be solved using textual cues alone and instead require genuine multimodal reasoning.

B. Task Design

Table 2 presents paired descriptions of conservation tasks and their matched non-conserving controls across all four quantitative properties, with corresponding illustrations in Figure 2.

Table 2. Task descriptions for conservation and non-conserving control scenarios across four quantitative properties.

Property	Conservation Task	Non-conserving Control
Number	Two rows of identical coins are presented in an initial configuration. One row is then spread apart without adding or removing any coins.	Two rows of identical coins are presented in an initial configuration. One row is then spread apart, with one coin added to said row.
Length	Two straws of identical length are shown in an initial configuration. One of the straws is then repositioned without altering its actual length.	Two straws of identical length are shown in an initial configuration. One of the straws is then repositioned while its actual length is altered (extendable straws are used).
Volume	A fixed volume of liquid is poured from one container into another of a different shape. Although the height changes significantly, the volume remains constant throughout the transformation.	A fixed volume of liquid is poured from one container into another of a different shape. A significant portion of water is left in the original container instead of being completely poured in.
Size	A lump of playdough is reshaped from one form (e.g., a ball) into another (e.g., a flattened disc). While the shape and surface features change, the total mass remains the same across both states.	A lump of playdough is reshaped from one form (e.g., a ball) into another (e.g., a flattened disc). A significant portion of playdough is left in the experimenter’s hand without being integrated into the new shape.

C. Prompting Strategy

Reasoning about conservation often requires interpreting the transformation as a continuous process across the videos or sequence of frames. To examine how prompts influence temporal integration and transformation-based reasoning, we design four prompt types, each progressively enhancing the model’s awareness of the underlying continuous process, as summarized in Table 3.

Together, these prompting strategies enable us to evaluate how different forms of linguistic scaffolding shape model engagement with visual dynamics. The “Sequential” and CoT prompts encourage frame-by-frame perception with step-by-step reasoning, directing attention to frame-wise visual evidence. In contrast, the “Continuous” prompt explicitly presents the multi-frame input as a continuous process, offering a conceptual cue to support conservation reasoning.

Table 3. Four different prompt formats used in our benchmark.

Prompt Type	Prompt Example
Direct Question	Is the number of coins in the upper row the same as in the lower row in the final image?
”Sequential” Prompt	Please process the images below sequentially, and then answer: Is the number of coins in the upper row the same as in the lower row in the final image?
CoT Prompt	Please process the images below sequentially. First describe what happens across the images, then answer: Is the number of coins in the upper row the same as in the lower row in the final image?
”Continuous” Prompt	The above images represent a continuous process. Please answer: Is the number of coins in the upper row the same as in the lower row in the final image?

D. Example Input

To provide clarity on the exact format of inputs provided to models, we present a complete example task below, including both the visual frames and the full textual prompt.

Task: Conservation of Number (Conserving condition)

Task Configuration: This example demonstrates a Number conservation task using Uniform extraction method with 7 frames and Direct Question prompt format.

Visual Input: The model receives a sequence of frames extracted from the video in temporal order (Frame 1 through Frame 7), ensuring that the transformation process is presented chronologically without any frame order disruption. Figure 6 shows an example with 7 frames, where frames are sampled uniformly across the video timeline. The first frame shows the initial state (two rows of coins with equal numbers), intermediate frames capture the transformation process (spreading one row), and the final frame shows the end state (one row spread out while maintaining the same number of coins).

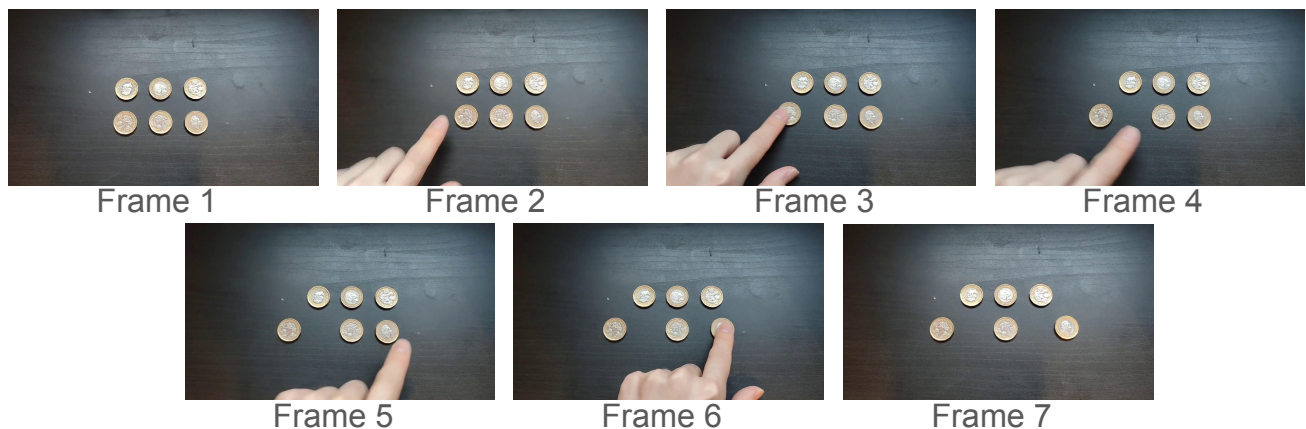


Figure 6. Example visual input: A sequence of 7 frames from a number conservation task, showing the initial state, transformation process, and final state.

Textual Input: Below is the structure of the prompt provided to the model (using the ”Direct Question” format). The [Image] placeholders indicate where the corresponding frames from Figure 6 are embedded in the actual input:

```

Frame 1: [Image]
Frame 2: [Image]
Frame 3: [Image]
Frame 4: [Image]
Frame 5: [Image]
Frame 6: [Image]

```

Frame 7: [Image]

Is the number of coins in the upper row the same as in the lower row in the final image?

Please choose one of the following options:

- (A) No, the lower row has more coins.
- (B) No, the upper row has more coins.
- (C) Yes, they are the same.

Ground Truth: Option (C) - Yes, they are the same.

Alternative Prompt Formats: For other prompt types, the question is prefixed with additional instructions. For example, the "Sequential" format would begin with "Please process the images below sequentially, and then answer: [question]", while the CoT format would include "Please process the images below sequentially. First describe what happens across the images, then answer: [question]". See Table 3 for details on all four prompt formats.

E. Model Inference

We evaluate 112 VLMs spanning diverse architectures, training regimes, and parameter scales, including mainstream proprietary models as well as advanced open-source models ranging from 1B to 76B parameters. Inference is conducted on a cluster equipped with 8× NVIDIA H100 (80 GB) GPUs. As a practical policy, models of 1–13B parameters typically run on a single GPU; 13–32B on two GPUs; 32–70B on four GPUs; and >70B on all eight GPUs.

To preserve fidelity and reproducibility, we adhere to configurations and reference implementations from the official codebases, avoiding unnecessary modifications. We build a scalable evaluation framework supporting parallel execution and compartmentalized environments. Inference jobs are distributed across GPUs via a dynamic scheduler that maximizes utilization and minimizes idle time. We additionally develop a lightweight modality-verification suite that prompts each model to summarize the media information it receives, and then the responses are checked by human reviewers to verify correct input routing and modality handling in our inference pipelines.

F. Evaluation

Rule-based template matching degrades with complex model outputs, yielding elevated false positives/negatives and requiring continual template optimization to cover corner cases. LLM-based matching better identifies intended choices within free-form text but can hallucinate, especially when brief answers are embedded in extensive context. To balance these trade-offs, we introduce Hybrid Matching, which prioritizes deterministic template matching and, on failure, falls back to an ensemble of four LLM judges (Qwen2.5-72B-Instruct, Mixtral-8x7B-Instruct-v0.1, DeepSeek-R1-Distill-Llama-70B, and Llama-3.1-70B). The ensemble decision is accepted only if at least three of four models return a consistent extraction; otherwise, the mapping is deemed unsuccessful. By coupling the precision of template extraction with the semantic flexibility of LLM adjudication, Hybrid Matching delivers more reliable mappings across diverse response styles.

G. Counterbalancing Conditions

Complete counterbalancing parameters and their factorial combinations for all four quantitative property domains are provided in Table 4.

Table 4. Counterbalanced variations of task-irrelevant features. Each unique combination of parameter values yields 48 distinct task instances per domain.

Domain	Parameter	Variations
Number	P1: Object Type	2 variants (Uniform, Mixed)
	P2: Mapping Shift	2 variants (Lower vs. Upper row moved)
	P3: Distance Spread	2 variants (Near, Far)
	P4: Number of Objects	6 variants (3–8 coins)
	Total combinations:	$2 \times 2 \times 2 \times 6 = 48$
Length	P1: Object Type	2 variants (Uniform, Mixed)
	P2: Mapping Shift	2 variants (Lower vs. Upper straw moved)
	P3: Distance Moved	2 variants (Near, Far)
	P4: Direction	2 variants (Left, Right)
	P5: Transformation Action	3 variants (Slide, Rotate, Vertical)
Total combinations:	$2 \times 2 \times 2 \times 2 \times 3 = 48$	
Volume	P1: Liquid Color	8 variants
	P2: Glass Transaction	2 variants (Tall \rightarrow Short, Short \rightarrow Tall)
	P3: Liquid Volume	3 variants (Small, Medium, Large)
	Total combinations:	$2 \times 8 \times 3 = 48$
Size	P1: Object Color	8 variants
	P2: Shape Transformation	6 variants (Crossing Sphere, Cylinder, Plane)
	Total combinations:	$6 \times 8 = 48$

H. Complete Model Results Aggregated Across Domains and Conditions

Complete performance metrics for all 112 evaluated VLMs, ranked by average accuracy, are provided in Tables 5 and 6.

Table 5. Complete Model Rankings by Average Accuracy (Ranks 1-56)

Rank	Model	Conserve (%)	Non-Conserve (%)	Average (%)	Strict (%)
0	Human Baseline	98.55	98.15	98.35	96.72
1	gemini-2.5-pro	94.33	43.88	69.11	41.20
2	doubao-seed-1.6-vision	82.99	46.42	64.71	38.22
3	gpt-5	91.48	35.82	63.65	33.14
4	claude-sonnet-4-5	75.43	45.39	60.41	37.23
5	Qwen-3-VL-32B-Instruct	64.57	52.06	58.31	31.15
6	Qwen-2.5-VL-72B-Instruct	89.69	21.98	55.83	17.32
7	hunyuan-t1-vision	74.05	36.05	55.05	26.80
8	InternVL-3-38B-Instruct	61.29	46.36	53.83	29.74
9	InternVL-3.5-38B-Instruct	75.49	31.80	53.64	19.32
10	InternVL-3.5-38B-MPO	72.75	33.98	53.36	20.85
11	InternVL-3-38B	57.47	48.42	52.95	29.41
12	InternVL-2.5-78B	60.71	44.43	52.57	19.27
13	Qwen-2.5-VL-32B-Instruct	81.82	22.83	52.33	16.66
14	InternVL-3.5-8B	72.53	29.93	51.23	15.62
15	Qwen-2-VL-72B-Instruct	69.44	31.52	50.48	15.24
16	InternVL-3.5-8B-Instruct	74.53	26.06	50.30	15.45
17	InternVL-2.5-38B	64.97	35.57	50.27	19.12
18	InternVL-2.5-78B-MPO	55.97	44.39	50.18	23.42
19	InternVL-3.5-8B-MPO	73.87	26.25	50.06	15.28
20	InternVL-3.5-1B-MPO	96.39	2.46	49.42	1.60
21	InternVL-3.5-1B-Instruct	93.45	3.45	48.45	1.96
22	InternVL-2-2B	77.56	18.13	47.85	8.16
23	Ovis1.6-Gemma2-9B	74.24	20.23	47.24	7.26
24	InternVL-3-14B-Instruct	74.86	19.24	47.05	8.94
25	Qwen-3-VL-32B-Thinking	61.44	32.44	46.94	20.23
26	InternVL-3.5-30B-A3B-MPO	75.13	17.29	46.21	9.15
27	InternVL-3-14B	69.07	22.90	45.99	11.00
28	Qwen-2-VL-7B-Instruct	66.58	25.14	45.86	6.20
29	InternVL-3.5-30B-A3B-Instruct	77.19	14.47	45.83	6.84
30	InternVL-2.5-38B-MPO	50.52	41.09	45.81	20.24
31	InternVL-2-40B	43.35	47.93	45.64	14.50
32	Qwen-2.5-VL-3B-Instruct	76.93	14.25	45.59	2.89
33	InternVL-2.5-1B-MPO	76.47	14.52	45.49	5.07
34	InternVL-2-26B	73.85	16.26	45.05	5.15
35	InternVL-3-2B-Instruct	81.51	7.93	44.72	1.50
36	R1-Onevision-7B	67.66	21.74	44.70	13.49
37	InternVL-3.5-1B	81.93	6.74	44.33	3.06
38	Phi-3.5-vision-instruct	71.53	17.12	44.32	5.35
39	InternVL-3-2B	76.01	12.05	44.03	2.75
40	InternVL-2.5-2B	59.59	28.25	43.92	10.89
41	InternVL-2.5-4B-MPO	77.03	10.63	43.83	6.55
42	llava-onevision-qwen2-7b-si-hf	58.76	27.93	43.34	3.40
43	InternVL-2-8B	74.09	12.07	43.08	4.12
44	Qwen-2.5-VL-7B-Instruct	64.12	21.55	42.83	7.39
45	llava-next-interleave-qwen-7b-dpo	50.13	35.20	42.66	6.17
46	InternVL-2-Llama3-76B	55.67	29.24	42.46	11.90
47	Qwen-3-VL-8B-Instruct	53.12	31.52	42.32	8.59
48	InternVL-3-8B-Instruct	70.95	13.61	42.28	7.97
49	InternVL-2.5-1B	74.86	9.41	42.14	3.69
50	InternVL-3-9B-Instruct	51.41	32.72	42.07	7.41
51	Mini-InternVL-Chat-4B-V1-5	79.77	4.24	42.01	0.75
52	InternVL-3.5-4B-Instruct	57.07	26.51	41.79	8.13
53	InternVL-3-9B	50.46	32.88	41.67	7.90
54	Qwen-2.5-Omni-3B	80.22	3.06	41.64	1.48
55	VLAA-Thinker-Qwen2VL-2B	48.60	34.20	41.40	5.31
56	InternVL-2-4B	78.26	4.22	41.24	1.76

Vision Language Models Cannot Reason About Physical Transformation

Table 6. Complete Model Rankings by Average Accuracy (Ranks 57-112, cont.)

Rank	Model	Conserve (%)	Non-Conserve (%)	Average (%)	Strict (%)
57	InternVL-3-8B	65.55	16.74	41.14	8.12
58	InternVL-3.5-4B	59.04	22.43	40.73	8.73
59	Phi-3-vision-128k-instruct	57.61	23.54	40.58	6.28
60	InternVL-2.5-4B	72.66	8.06	40.36	4.66
61	Qwen-2.5-Omni-7B	66.48	14.11	40.30	7.84
62	VLAA-Thinker-Qwen2.5VL-7B	54.77	25.56	40.16	10.56
63	InternVL-2.5-26B	47.66	32.42	40.04	9.60
64	Qwen-2-VL-2B-Instruct	44.73	34.68	39.70	4.33
65	InternVL-3-78B-Instruct	45.27	33.92	39.60	15.14
66	InternVL-3-78B	43.04	35.90	39.47	15.97
67	VLAA-Thinker-Qwen2VL-7B	52.68	25.69	39.18	7.84
68	InternVL-3.5-14B-Instruct	42.58	35.31	38.95	9.46
69	InternVL-3.5-38B	58.69	19.16	38.92	11.28
70	InternVL-3.5-4B-MPO	52.60	25.08	38.84	7.67
71	Qwen-3-VL-2B-Instruct	50.82	25.99	38.40	5.62
72	llava-onevision-qwen2-7b-ov-hf	47.35	29.06	38.21	2.07
73	llava-onevision-qwen2-7b-ov-chat-hf	47.64	28.40	38.02	2.01
74	InternVL-Chat-V1-5	52.10	23.64	37.87	6.76
75	InternVL-3.5-2B	63.97	11.61	37.79	4.23
76	InternVL-3.5-2B-Instruct	62.85	12.32	37.58	4.46
77	xgen-mm-phi3-mini-instruct-interleave-r-v1.5	57.61	17.35	37.48	2.33
78	InternVL-3.5-2B-MPO	61.43	12.76	37.10	4.31
79	InternVL-2.5-26B-MPO	34.80	38.07	36.44	9.70
80	Mini-InternVL-Chat-2B-V1-5	42.32	29.75	36.03	2.67
81	Phi-4-multimodal-instruct	33.79	36.94	35.36	5.45
82	InternVL-2.5-8B	47.28	23.09	35.19	5.82
83	Qwen-3-VL-4B-Instruct	49.05	20.83	34.94	6.77
84	Qwen-3-VL-8B-Thinking	52.92	16.31	34.61	7.42
85	InternVL3.5-GPT-OSS-20B-A4B-Preview	57.01	11.61	34.31	4.64
86	VLAA-Thinker-Qwen2.5VL-3B	36.44	31.66	34.05	9.13
87	Mantis-llava-7b	31.46	36.21	33.83	4.23
88	InternVL-2.5-8B-MPO	37.53	29.13	33.33	7.42
89	InternVL-2.5-2B-MPO	32.20	34.24	33.22	4.92
90	llava-v1.6-mistral-7b-hf	33.33	32.85	33.09	0.00
91	InternVL-3-1B	52.17	13.98	33.07	0.47
92	InternVL-3-1B-Instruct	52.93	13.09	33.01	0.25
93	InternVL-Chat-V1-1	23.54	42.34	32.94	2.45
94	Mantis-8B-Idedics2	29.57	36.30	32.93	1.48
95	llama3-llava-next-8b-hf	32.44	32.47	32.45	0.00
96	llava-onevision-qwen2-0.5b-si-hf	19.06	41.86	30.46	1.10
97	llava-onevision-qwen2-0.5b-ov-hf	3.70	54.84	29.27	0.54
98	Qwen-3-VL-4B-Thinking	40.77	17.66	29.21	6.73
99	Mantis-8B-clip-llama3	18.65	39.71	29.18	2.79
100	Mantis-8B-siglip-llama3	12.33	43.78	28.05	1.47
101	InternVL-3.5-30B-A3B	47.53	8.47	28.00	4.92
102	Xinyuan-VL-2B	11.82	44.11	27.97	3.20
103	Mantis-8B-Fuyu	20.31	35.07	27.69	0.36
104	InternVL-Chat-V1-2	11.11	43.85	27.48	2.93
105	InternVL-Chat-V1-2-Plus	0.71	51.53	26.12	0.28
106	Mantis-bakllava-7b	17.10	34.44	25.77	1.15
107	InternVL-2-1B	3.04	47.55	25.30	0.34
108	JanusFlow-1.3B	29.39	20.25	24.82	1.76
109	Janus-Pro-7B	28.66	20.89	24.78	2.74
110	Janus-1.3B	29.05	17.61	23.33	0.66
111	Janus-Pro-1B	19.51	23.62	21.57	1.42
112	Qwen-3-VL-2B-Thinking	30.10	9.52	19.81	2.51

I. Combined Model Performance By Quantitative properties

Average Accuracy by Domain: Conservation Task vs Non-Conserving Control

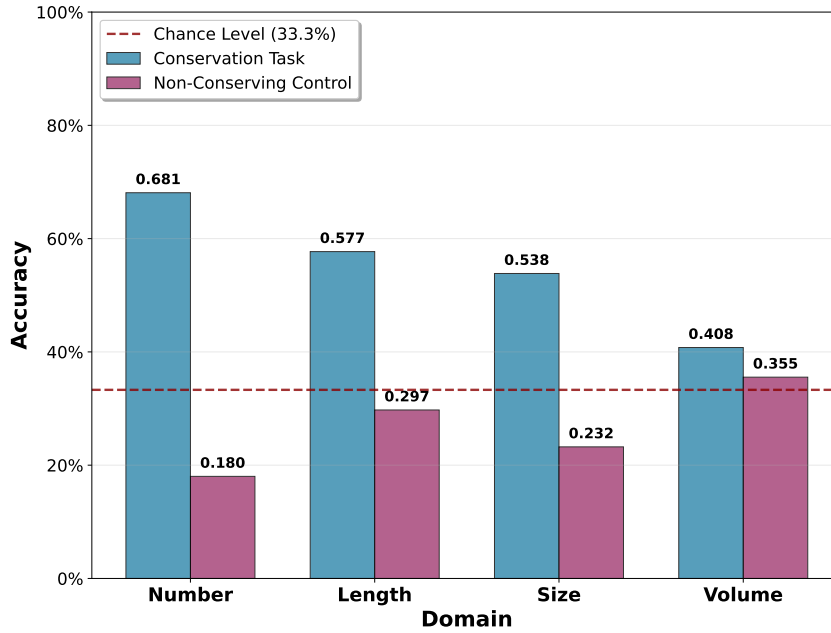


Figure 7. Average model performance by quantitative domains. Models consistently perform worse on non-conserving controls compared to conservation tasks.

J. Model response under empty image and text control

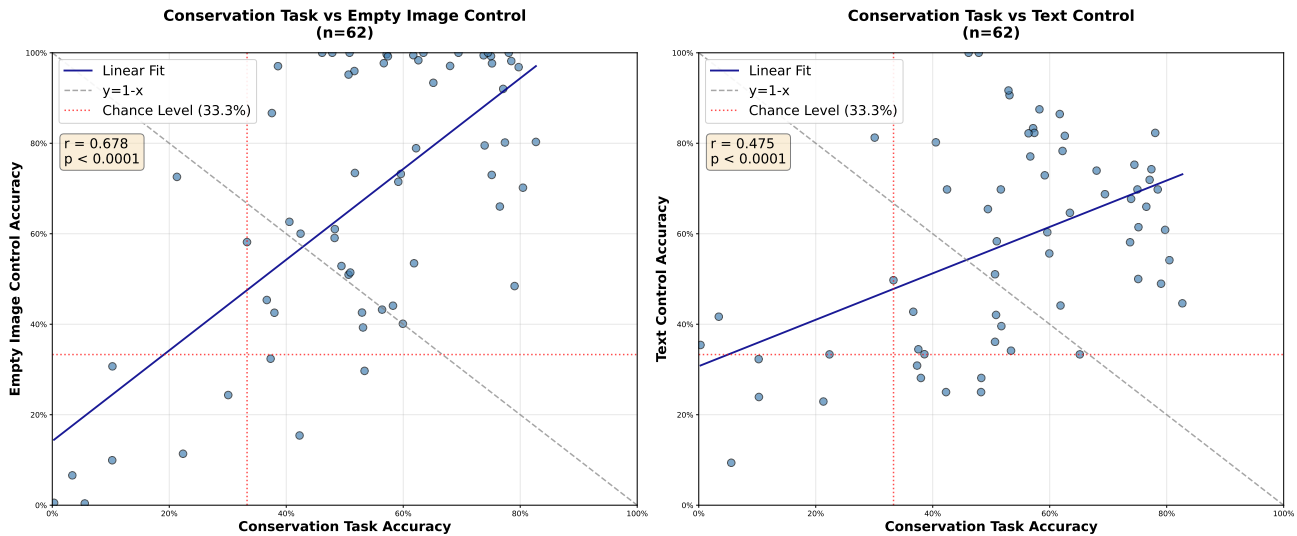


Figure 8. Model-level correlations between conservation task performance and control condition biases. (Left) Conservation task accuracy versus Empty Image Control accuracy shows strong positive correlation ($r = 0.578$, $p < 0.0001$), indicating models performing better on conservation tasks exhibit stronger textual priors favoring quantity invariance when visual content is removed. (Right) Conservation task accuracy versus Text Control accuracy shows similar but slightly weaker correlation ($r = 0.475$, $p < 0.0001$), with both patterns demonstrating that success on conservation tasks is driven primarily by textual biases rather than visual transformation reasoning. Evaluated on 62 VLMs supporting both empty image and text-only inputs under 7-frame conditions.